

# High Resolution Multi-slice Myocardial $T_2$ Mapping with Improved Scan Time Efficiency

Jihye Jang<sup>1,2</sup>, Cory Tschabrunn<sup>1</sup>, Elad Anter<sup>1</sup>, Tamer Basha<sup>1</sup>, and Reza Nezafat<sup>1</sup>

<sup>1</sup>Beth Israel Deaconess Medical Center and Harvard Medical School, Boston, Massachusetts, United States, <sup>2</sup>Computer Aided Medical Procedures, Technische Universität München, Munich, Bayern, Germany

**Introduction/ Purpose:** Quantitative myocardial  $T_2$  mapping allows non-invasive assessment of myocardial inflammation and edema [1]. In a typical  $T_2$  mapping sequence, pixel-wise  $T_2$  maps are generated by acquiring series of  $T_2$  weighted images with different  $T_2$  prep echo times using an ECG triggered single-shot acquisition. Rest cycles are needed between each two successive images to allow full magnetization recovery, which results in a reduced scan time efficiency. In such sequence, multi-segment acquisition is difficult to be employed as it requires even more rest cycles between each two successive segments, which makes the scan time even longer. This reduces the feasibility of the multi-segment high-resolution  $T_2$  mapping in clinical settings. Recently, a free-breathing multi-slice myocardial  $T_2$  mapping sequence was proposed to increase the scan time efficiency of  $T_2$  mapping sequence by combining a slice-selective  $T_2$  prep pulse and interleaved slice acquisition which eliminates the need of rest cycles for magnetization recovery. In this study, we sought to further extend the multi-slice  $T_2$  mapping sequence to allow segmented acquisition to achieve higher in-plane spatial resolution within an acceptable scan time.

## Methods

**Imaging Sequence:** **Fig. 1** shows the schematic of the proposed segmented data acquisition for multi-slice myocardial  $T_2$  mapping, which consists of multiple slice-selective  $T_2$  prep prepared blocks with different echo times. Each block is acquired using an ECG triggered multi-shot acquisition, which is repeated for all k-space segments. This acquisition block is then repeated with different order of slices to acquire all slices at each echo time.

**Experimental Validation:** To characterize the proposed sequence in terms of accuracy, precision, and reproducibility, vials of  $\text{NiCl}_2$  doped agarose phantom with different  $T_1/T_2$  times were imaged five times repeatedly using a segmented data acquisition scheme and compared to a single-shot multi-slice  $T_2$  mapping sequence (*single-shot*:  $\text{TR/TE}=2.7/1.3\text{ms}$ , voxel size= $2\times 2\text{mm}^2$ , slice thickness= $8\text{mm}$ , TFE factor=73, acquisition window= $195.8\text{ms}$ / 3-segments:  $\text{TR/TE}=3.8/1.9\text{ms}$ , voxel size= $1\times 1\text{mm}^2$ , slice thickness= $10\text{mm}$ , TFE factor=36, acquisition window= $136.9\text{ms}$ , with bSSFP imaging readout, flip angle=85,  $\text{FOV}=280\times 280\text{mm}^2$ , linear k-space ordering, 10 linear ramp-up pulses, SENSE factor=2). Accuracy was defined as the difference between the mean  $T_2$  value and the averaged reference  $T_2$  (spin echo) in each vial. Precision was defined as the averaged standard deviation of  $T_2$  in each vial. Reproducibility was defined as the standard deviation of  $T_2$  over five repetitions. Statistical significances between sequences were assessed using a Wilcoxon signed rank test. To evaluate the spatial resolution, images were acquired using a high resolution phantom with single-shot, 3-segments, 5-segments acquisition which results in  $2\times 2\text{mm}^2$ ,  $1\times 1\text{mm}^2$ ,  $0.7\times 0.7\text{mm}^2$  in-plane spatial resolution, respectively (*single-shot*:  $\text{TR/TE}=2.7/1.4\text{ms}$ , voxel size= $2\times 2\text{mm}^2$ , slice thickness=8mm, TFE factor=106, acquisition window=285ms/ 3-segments:  $\text{TR/TE}=3.8/1.9\text{ms}$ , voxel size= $1\times 1\text{mm}^2$ , slice thickness=10mm, TFE factor=60, acquisition window=229ms/ 5-segments:  $\text{TR/TE}=4.8/2.4\text{ms}$ , voxel size= $0.7\times 0.7\text{mm}^2$ , slice thickness=10mm, TFE factor=50, acquisition window=239ms, with bSSFP imaging readout, flip angle=85,  $\text{FOV}=380\times 412\text{mm}^2$ , linear k-space ordering, 10 linear ramp-up pulses, SENSE factor=2). To further investigate the feasibility of the proposed multi-shot sequence, an ex-vivo heart of an infarcted swine model were imaged using a multi-slice  $T_2$  mapping sequence with different number of segments in k-space (*single-shot*:  $\text{TR/TE}=2.9/1.4\text{ms}$ , voxel size= $2\times 2\text{mm}^2$ , slice thickness=8mm, TFE factor=41, acquisition window=117.5ms/ 3-segments:  $\text{TR/TE}=3.9/1.95\text{ms}$ , voxel size= $1\times 1\text{mm}^2$ , slice thickness=10 mm, TFE factor=23, acquisition window=89.7ms/ 5-segments:  $\text{TR/TE}=6.1/3\text{ms}$ , voxel size= $0.5\times 0.5\text{mm}^2$ , slice thickness=10mm, TFE factor=26, acquisition window=158ms, with bSSFP imaging readout, flip angle=85,  $\text{FOV}=200\times 152\text{mm}^2$ , linear k-space ordering, 10 linear ramp-up pulses, SENSE factor=2).  $T_2$  maps were generated by voxel-wise curve-fitting of the signal with a three-parameter fit model [2].

**Results:** In phantom study, the multi-shot  $T_2$  mapping sequence provides similar accuracy and reproducibility ( $p>0.05$ ) with lower precision ( $p=0.002$ ) compared to a single-shot sequence (**Fig. 2**). The impact of the improved spatial resolution was shown in the phantom study (**Fig. 3**), as well as in the ex-vivo study (**Fig. 4**).

**Conclusion:** The proposed high resolution multi-slice  $T_2$  mapping using segmented data acquisition allows higher in-plane spatial resolution with high efficiency in the scan time.

**Acknowledgements:** Grant support from NIH R01EB008743 and Samsung Electronics.

**References:** [1] He, JMRI, 2006, [2] Akçakaya, MRM, 2014.

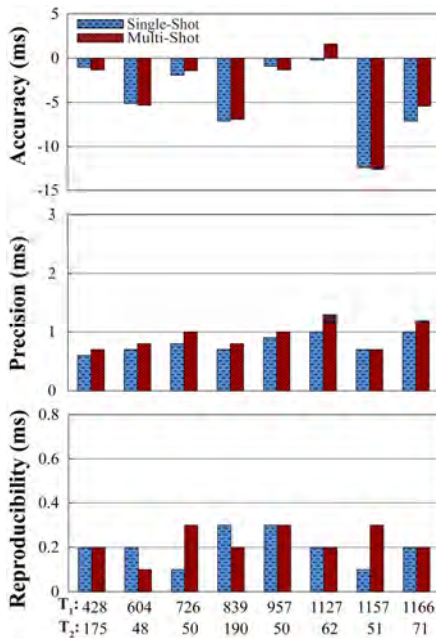


**Figure 2.** Multi-shot sequence yields similar accuracy and reproducibility with reduced precision compared to the single-shot multi-slice myocardial  $T_2$  mapping sequence in the phantom study.

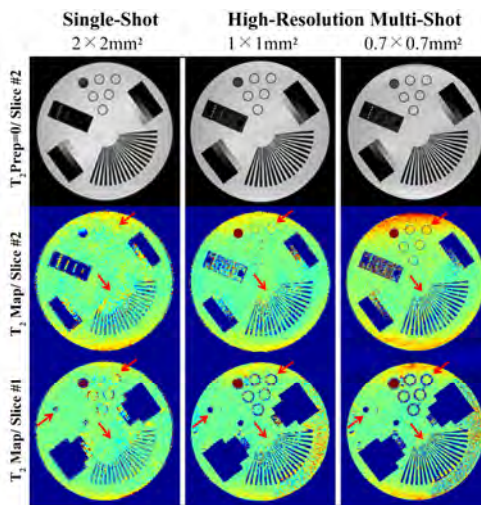


**Figure 3.** Different phantom structures appear sharper in the high resolution  $T_2$  maps acquired using the multi-slice acquisition compared to the single-shot sequence.

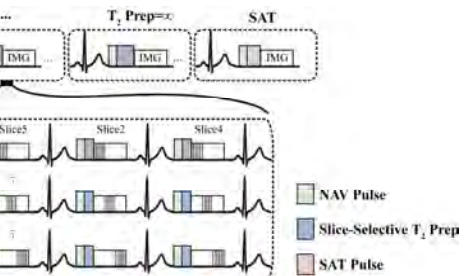


**Figure 1.** Schematic of the high resolution multi-slice  $T_2$  mapping sequence using segmented data acquisition. A series of  $T_2$  prep blocks (First block:  $T_2$  prep=0, last block:  $T_2$  prep=∞) which acquired after saturation pulse are acquired using a segmented data acquisition and repeated with different order of slices.

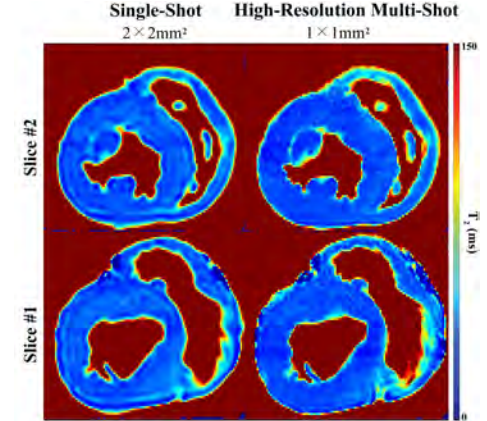


**Figure 4.** Two representative slices of  $T_2$  maps acquired from an ex-vivo infarcted heart of a swine model. Reduced partial voluming error is shown on the high-resolution  $T_2$  maps which are acquired using the proposed multi-slice  $T_2$  mapping sequence.